



ELSEVIER

Available online at [www.sciencedirect.com](http://www.sciencedirect.com)

SCIENCE @ DIRECT®

Composites: Part A 35 (2004) 827–840

**composites**

Part A: applied science  
and manufacturing

[www.elsevier.com/locate/compositesa](http://www.elsevier.com/locate/compositesa)

## A comparison between the Iosipescu and off-axis shear test methods for the characterization of *Pinus Pinaster Ait*

J.C. Xavier<sup>a</sup>, N.M. Garrido<sup>b</sup>, M. Oliveira<sup>b</sup>, J.L. Morais<sup>a,\*</sup>, P.P. Camanho<sup>c</sup>, F. Pierron<sup>d</sup>

<sup>a</sup>CETAV/UTAD, Departamento de Engenharias, Quinta de Prados, 5001-901 Vila Real, Portugal

<sup>b</sup>DEMAD/ESTV, Campus Politécnico, Repeses, 3504-510 Viseu, Portugal

<sup>c</sup>DEMEGI/FEUP, Rua Dr Roberto Frias, 4200-465 Porto, Portugal

<sup>d</sup>LMPF/ENSAM, Rue Saint-Dominique, BP 508, 51006 Châlons-en-Champagne, France

### Abstract

In this work, the applicability of the Iosipescu and off-axis test methods for the shear characterization of clear wood was investigated. Wood of maritime pine (*Pinus Pinaster Ait.*) was used. Iosipescu shear tests were carried out for oriented specimens in the three natural symmetry planes of wood (LR, LT and RT planes), whereas off-axis tests were performed only in the LR and LT planes. Finite element analyses were conducted in order to access the stress and strain fields in the test section of the specimens. It was found that the Iosipescu and off-axis tests provide different shear moduli values. It was also shown that the Iosipescu test gives lower and upper bounds of shear strengths, whereas the off-axis test gives only a lower bound, directly from the measured loads.

© 2004 Elsevier Ltd. All rights reserved.

**Keywords:** A. Wood; B. Mechanical properties; C. Finite element analysis (FEA); D. Mechanical testing

### 1. Introduction

The accurate knowledge of the mechanical properties of solid wood is a fundamental requirement for its utilization as a competitive structural material. However, the experimental identification of the mechanical behaviour of wood remains an open problem, due to its natural variability, heterogeneity and anisotropy.

It is commonly admitted that wood is orthotropic, with three orthotropic planes of symmetry for its internal structure. These planes are defined by longitudinal direction (L) along fibres, radial direction (R) parallel to the rays, and tangential direction (T) to the growth rings. The mechanical behaviour of wood is completely characterized by the stress–strain relationships referred to the LRT reference frame. Such relationships are necessary for an efficient and safe design of wooden structural members or joints, where the stress and strain fields can be quite complex [1–3]. Even in a structural member with a simple global shape and loading, the stress

and strain distributions can be very complex because of grain deviations or knots [4,5].

The mechanical tests are the only way to determine the stress–strain response of wood, but several difficulties arise in performing the right experimental measurements, which are yet unresolved. The main problem to overcome is the identification of the shear response in the principal material planes (LR, LT and RT planes), including the identification of shear strengths. The current standard test methods for measurement of the shear properties of clear wood have serious limitations and drawbacks. It is broadly recognized that a shear test method that can evaluate both all the shear moduli and shear strengths of clear wood, should be standardized as soon as possible [6].

During the last decades, an intensive research effort has been devoted to the experimental identification of shear properties of orthotropic synthetic composite materials. Different shear test methods have been proposed, among which are the Iosipescu shear test and the off-axis tensile test. The Iosipescu shear test was first developed for measuring the shear strength of metal rods [7], and has been studied extensively by the composite research community within the last 20 years, starting with the work of Walrath and Adams [8] in the early eighties. The fixture developed by Adams and Walrath [9], known

\* Corresponding author. Tel.: +351-259-350-306; fax: +351-259-350-356.

E-mail address: [jmorais@utad.pt](mailto:jmorais@utad.pt) (J.L. Morais).

as the ‘modified Wyoming fixture’, was included in an ASTM Standard (D 5379-93) [10] and is widely used in composite research laboratories. An alternative fixture design was proposed by Pierron [11], in order to overcome a certain number of drawbacks of the ‘modified Wyoming fixture’. The so-called EMSE (Ecole des Mines de Saint-Etienne) fixture is based on the same specimen geometry but with a different load-introduction system, designed to eliminate parasitic in-plane and out-of-plane movements.

The majority of works about the Iosipescu shear test addressed the problem of correct measurement of shear modulus and shear strength of synthetic composite materials. The first issue is more or less a solved problem [12], however the second one is far from being solved [13,14]. There are very few studies about the applicability of the Iosipescu shear test to clear wood [6,15–17].

The off-axis tensile test has been used for a number of years to determine the in-plane shear response of advanced composite materials [18–22]. An inherent difficulty in this test method is the extension-shear coupling resulting from the anisotropic material behaviour [19]. Indeed, owing to the end-constraint effects, heterogeneous stress and strain fields develop in the gauge section of the off-axis specimens, which can lead to their premature failure and inaccurate shear modulus measurements. One way to surmount these difficulties when measuring the shear modulus is to use correction factors. Another way involves the modification of the test configuration in order to produce a homogeneous stress and strain distribution throughout the gauge section of the specimens. A procedure of this type was proposed by Sun and Chung [20], based on oblique end tabs. Pierron and Vautrin [21] have studied this solution, confirming a state of approximately uniform stress and strain, and the potential of using oblique end tabs to measure the shear strength. The few studies about the off-axis tensile test of clear wood are mainly dedicated to the identification of shear properties in the LR principal material plane [23,24].

The purpose of this paper is to present a comparison between the Iosipescu and off-axis test methods for the shear characterization of clear wood, in its principal material planes. This will include a finite element study and presentation of experimental results to compare the two shear-test methods in terms of shear moduli and shear strengths.

## 2. Data reduction

The objective of this section is to perform a brief review of data reduction procedures for the measurement of shear properties of orthotropic materials using the Iosipescu shear test and the off-axis tensile test.

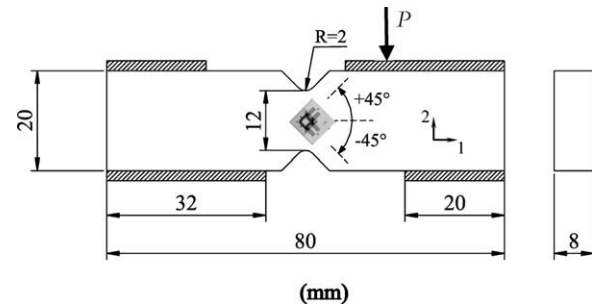


Fig. 1. Configuration of the Iosipescu specimens.

### 2.1. Iosipescu test

The Iosipescu specimen has the shape of a rectangular beam of small dimensions, with symmetric V-notches at its centre (Fig. 1). A suitable fixture is used in order to transform the applied load into a shear loading, acting at the specimen minimum cross-section area, between the V-notches. The geometry of the V-notches is such that a quasi uniform shear-stress distribution is produced at the centre of the specimen.

The shear strains are usually measured with two-element strain gauge rosettes, which average the strains over the area of the gauge grid. The rosettes are fixed at the centre of the specimens at  $\pm 45^\circ$  to their longitudinal axis (Fig. 1). The engineering shear strain in the principal material axes (1, 2) is given by

$$\varepsilon_6^{\text{av}} = \varepsilon_{+45^\circ} - \varepsilon_{-45^\circ}, \quad (1)$$

where  $\varepsilon_{+45^\circ}$  is the strain measured by the  $+45^\circ$  gauge and  $\varepsilon_{-45^\circ}$  is the strain measured by the  $-45^\circ$  gauge.

The average shear stress on the minimum specimen cross-section is as follows

$$\sigma_6^{\text{av}} = \frac{P}{A}, \quad (2)$$

where  $A$  is the area of the cross section between the notches and  $P$  is the global load applied to the specimen and measured by the load cell of the testing machine.

An apparent shear modulus can be calculated dividing the average shear stress by the engineering shear strain, provided that axes (1, 2) are principal material axes

$$G_{12}^{\text{a}} = \frac{\sigma_6^{\text{av}}}{\varepsilon_6^{\text{av}}}. \quad (3)$$

The apparent shear modulus will be the true shear modulus if the shear stress and strain distributions are uniform along the test section of the specimens. It is well known however, that such ideal condition is not achieved when testing anisotropic materials [12]. To account for the non-uniformity of the stress distribution between the notches, a correction factor  $C$  was defined as follows

$$C = \frac{\sigma_6}{\sigma_6^{\text{av}}}, \quad (4)$$

where  $\sigma_6$  is the shear stress at the central point of the specimen. In order to incorporate the difference between the engineering shear strain  $\varepsilon_6$  at the central point and the strain gauge reading, a correction factor  $S$  was defined as

$$S = \frac{\varepsilon_6^{\text{av}}}{\varepsilon_6}. \quad (5)$$

The apparent shear modulus evaluated directly from the experimental data Eq. (3) must be corrected by the factors  $C$  and  $S$  to get the true shear modulus

$$G_{12} = CSG_{12}^a. \quad (6)$$

Approximate values of stress and strain correction factors can only be achieved by finite element modelling.

The reduction procedure presented above is based on the implicit assumption of a uniform distribution of shear stress and strain through the thickness of the specimen. However, as pointed out by Pierron [12], the strains measured on both faces of the same specimen can be quite distinct due to the heterogeneity of the applied loading, caused by geometrical imperfections of the loading faces of the specimen. It was shown by the author that the scatter of the results due to such an effect can be eliminated by averaging the shear strains on the two faces of the specimen.

The ultimate shear stress carried out by the specimens can be defined as

$$\sigma_6^{\text{ult}} = \frac{P_f}{A}, \quad (7)$$

where  $P_f$  is the applied load at the occurrence of failure. In the field of synthetic composite materials, there is a debate about what the failure load in the Iosipescu test is. Moreover, the shear stress state is not pure over the gauge section of the Iosipescu coupon, and therefore the ultimate shear stress defined above Eq. (7) cannot be interpreted as the material shear strength. Despite these facts, Pierron and Vautrin [13] have demonstrated, for a unidirectional T300/914 composite, that a correct evaluation of the shear strength can be made using a failure criterion that takes into account the presence of compressive transverse stresses.

## 2.2. Off-axis test

In the off-axis tensile test, a rectangular orthotropic specimen with fibres oriented at a certain angle ( $\alpha$ ) with respect to the applied load, is subjected to a tensile loading (Fig. 2). The orthotropic nature of the material is used to

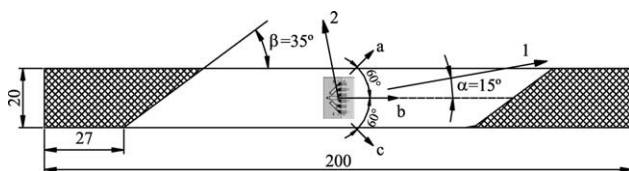


Fig. 2. Configuration of the off-axis specimens.

produce predominant shear behaviour in the material coordinate system (1, 2).

The shear strains are measured with three-element strain gauge rosettes, fixed at the centre of the off-axis specimens. The engineering shear strain in the principal material axes (1, 2),  $\varepsilon_6$ , is obtained by the appropriate transformation of the strain gauge readings. For the 60-deg-delta rosette glued in the specimen as illustrated in Fig. 2,  $\varepsilon_6$  is defined according to the following transformation equation

$$\varepsilon_6 = (\varepsilon_a - 2\varepsilon_b + \varepsilon_c)\sin \alpha + (\varepsilon_a - \varepsilon_c)\cos \alpha, \quad (8)$$

where  $\varepsilon_a$ ,  $\varepsilon_b$  and  $\varepsilon_c$  are the normal strain readings along the grid directions  $a$ ,  $b$  and  $c$ , respectively.

From the global load  $P$  applied to the off-axis specimen, and recorded by the load cell, the stresses in the principal material axis (1, 2), are obtained by stress transformation as follows

$$\begin{aligned} \sigma_1 &= \frac{P}{A} \cos^2 \alpha, \\ \sigma_2 &= \frac{P}{A} \sin^2 \alpha, \end{aligned} \quad (9)$$

$$\sigma_6 = -\frac{P}{A} \cos \alpha \sin \alpha,$$

where  $A$  is the cross-sectional area of the specimen.

The shear modulus is evaluated by dividing the shear stress Eq. (9) by the engineering shear strain Eq. (8)

$$G_{12} = \frac{\sigma_6}{\varepsilon_6}. \quad (10)$$

If the specimens have a high enough aspect ratio (length/width) and an appropriate off-axis angle is chosen, an almost uniaxial and uniform stress state in the specimen coordinate system ( $x, y$ ) and a predominant shear behaviour in the material coordinate system (1, 2) are expected. Moreover, as suggested by Sun and Chung [20], and confirmed by other authors [21,22], the use of oblique end tabs provides a more uniform state of stress in the specimens gauge section. The oblique angle  $\beta$  of the end tabs, relative to the longitudinal direction of the specimen, was calculated using the following formula [20,21]

$$\cot \beta = -\frac{\bar{S}_{16}}{\bar{S}_{11}}, \quad (11)$$

where  $\bar{S}_{ij}$  are the elements of the compliance matrix with respect to the specimen coordinate system ( $x, y$ ). Hence, with a suitable combination of those geometrical parameters, Eq. (10) is thought to provide the true shear modulus of the material being tested.

Pierron and Vautrin [21] have proved that the use of oblique end tabs significantly improves the measurement of the ultimate shear stress of off-axis specimens. The authors have shown the importance of taking into account the effect of the tensile transverse stress component in the shear

strength identification. Therefore, the shear strength can only be correctly identified by means of a failure criterion.

### 3. Experimental work

#### 3.1. Material and specimens

Mature wood of maritime pine (*Pinus Pinaster Ait.*) was used in this work. All test specimens were obtained from the same tree, about 74 years old, selected from a population in the district of Viseu (Portugal). One log, between 3 and 6 m above the basal plane, was quarter-sawn and plain-sawn into boards. These boards were dried in the kiln to between 10 and 12% moisture content.

In order to account for the variability of wood, matched specimens were manufactured from the boards for measuring the shear properties in the LR, LT and RT planes. After manufacturing, the test specimens were left into the laboratory during several days before testing, in order to reach their equilibrium state. The temperature and the relative humidity of the laboratory were  $23 \pm 1^\circ\text{C}$  and  $45 \pm 5\%$ , respectively. When the equilibrium condition was attained, the dimensions and mass of each specimen were determined. The moisture content was calculated after testing, according to the oven-dry method. The density was determined dividing the oven-dry mass by the volume of each specimen. The equilibrium moisture content, of all tested specimens, was between 10 and 12%, and the oven-dry density was between 0.501 and 0.623 g/cm<sup>3</sup>.

The nominal dimensions of the Iosipescu specimens are presented in Fig. 1. These dimensions are based on the ASTM D 5379-93 standard [10], for synthetic fibre composites. Several specimens were tested, oriented in the LR (nine specimens), LT (ten specimens) and RT (eight specimens) orthotropic planes.

The nominal dimensions of the off-axis specimens are presented in Fig. 2. The thickness of the specimens was taken as 4 mm. The nominal off-axis angle was chosen to be  $15^\circ$ , through a preliminary calculation based on the Chamis and Sinclair criterion [18], for both LR and LT specimens. The elastic properties used in this calculation were the principal elastic moduli of wood *Pinus Pinaster Ait.*, determined by Pereira [25] (Table 1), and the shear moduli of all wood pine species reported in reference [26]. The off-axis angle of each specimen was carefully checked after testing, using a microscope equipped with a goniometer.

Table 1  
Engineering elastic properties used in the finite element analyses

$E_L^a$ (GPa)	$E_R^a$ (GPa)	$E_T^a$ (GPa)	$\nu_{RT}^a$	$\nu_{TL}^a$	$\nu_{LR}^a$	$G_{RT}^b$ (GPa)	$G_{LT}^b$ (GPa)	$G_{LR}^b$ (GPa)
15.1	1.91	1.01	0.59	0.051	0.47	0.176	1.096	1.109

<sup>a</sup> Moduli of elasticity and Poisson's ratios of *Pinus Pinaster Ait.* [25].

<sup>b</sup> Shear moduli of *Pinus Taeda L.* [26].

Oblique end tabs, made from wood Kambala (*Chlorophora Excelsior Ait.*) with a nominal angle of  $36^\circ$ , were bonded on both ends of the specimens. The oblique tab angle was obtained according to Eq. (11), using the reference engineering elastic constants of Table 1. The results of a finite element analysis had shown that the difference between the reference and the actual shear moduli, at least within the range of shear modulus of wood pine species reported in the *Wood Handbook* [26], has a negligible effect on the oblique tab angle [28]. In the LR and LT planes, 16 and 14 specimens were tested, respectively. Off-axis tests on the RT plane were not considered because of the difficulty of making the test coupons due to the growth ring curvature. Moreover, the orthotropic ratio in this configuration is very low ( $E_R/E_T = 1.9$ ), making off-axis test an inefficient shear test.

#### 3.2. Iosipescu tests

The Iosipescu shear tests were run on an INSTRON 1125 universal testing machine, at a controlled displacement rate of 1 mm/min. The EMSE fixture was used. The fixture was mounted in an inverted position to fit the testing machine (Fig. 3), thus the specimens had a pre-load equal to the weight of the movable part of the fixture (about 14 N). The applied load was measured with a 5 kN load cell and each specimen was instrumented with two 0/90 rosettes (Micro-Measurement CEA-06-125WT-350), fixed back to back at  $\pm 45^\circ$  at the centre of the specimens (Fig. 1). The grid dimensions of the rosettes are  $3.18 \times 4.57 \text{ mm}^2$ . The gauge fixing procedure was that recommended by MicroMeasurement. Since posterior corrections with strain tensor transformation is not possible, the rosettes were positioned with great care, with the aid of an optical microscope equipped with a coordinate table and a goniometer. The force and strain outputs were recorded on a personal

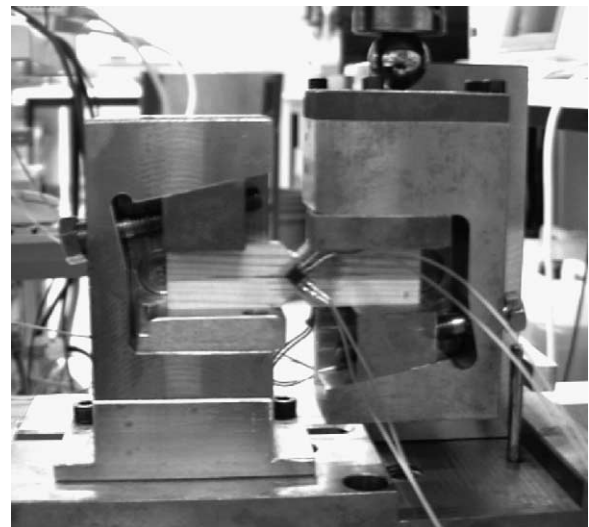


Fig. 3. Iosipescu fixture, based on the EMSE (Ecole de Mines de Saint-Etienne) design.



computer through a data acquisition system HBM SPIDER 8. The correction of the non-linearity of the quarter-bridge setup and the transverse-sensitivity of the strain gauges has been taken into account on data analysis and reduction.

After connecting the strain rosettes to the Wheatstone bridge, several minutes were taken in order to get a stable strain reading. Only after this stabilization, the electronic zero of the strain rosettes was set and the specimens mounted into the fixture. A torque wrench was used to tighten the sliding wedges of the fixture to a torque of 1 Nm. This value was a compromise between a torque too small that would allow sliding of the specimen with respect to the fixture, and a torque too large that could introduce high initial deformations and cause local crushing of the specimens.

Before testing, the LR and LT specimens were loaded and unloaded five times up to a force equal to about 300 N, in order to accommodate the specimens to the fixture. For the RT specimens, this load-unload cycles were not performed, due to their low strength.

### 3.3. Off-axis tests

The off-axis tensile tests were conducted in an INSTRON 1125 universal testing machine, with a crosshead speed of 1 mm/min. Wedge action grips were employed (Fig. 4), which promotes a rigid clamping condition of the specimen ends. The applied load was measured with a 100 kN load

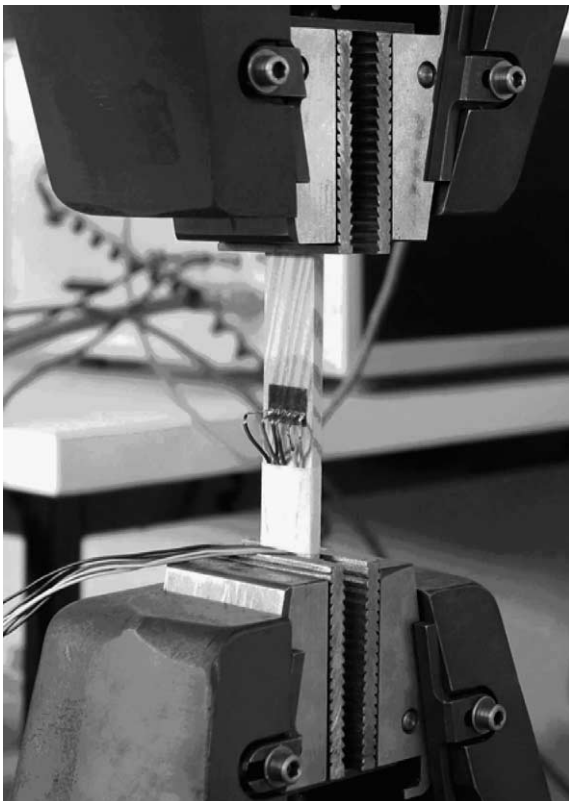


Fig. 4. Wedge action grips for the off-axis tensile tests.

cell. All specimens were instrumented with one 60-deg-delta rosette (MicroMeasurement CEA-06-125UR-350), bonded according the MicroMeasurement recommendations. The grid dimensions of the rosettes are  $3.18 \times 1.52 \text{ mm}^2$ . After testing, the alignment angles of the strain gauge rosettes with respect to the axes of symmetry of the specimens were carefully measured under a microscope with a goniometer, and recorded for data reduction. A similar testing methodology, data acquisition system and data reduction procedure was employed for the off-axis tensile tests as for the Iosipescu shear tests.

## 4. Finite element analyses

Numerical analyses of the Iosipescu and off-axis test methods were carried out using the finite element code ANSYS 6.0<sup>®</sup>. The purpose of these analyses was to access the stress and strain fields in the test sections of both the Iosipescu and off-axis specimens, and to determine the appropriate correction factors needed for the accurate identification of the shear moduli of wood by the Iosipescu test. Wood was considered as a linear elastic, orthotropic and homogeneous material, with the properties shown in Table 1. The geometry and dimensions of the Iosipescu and off-axis specimens are those used in the experimental work. The details of finite element analyses and results for the Iosipescu and off-axis tests can be found in Refs. [27,28], respectively.

### 4.1. Iosipescu shear test models and results

Assuming a plane stress approach, a 2D finite element model was created, which simulated the loading conditions of the EMSE fixture. The model uses the quadrilateral isoparametric element PLANE82, with eight nodes and a total of 16 degrees of freedom. The mesh, defined after a preliminary convergence study, and the boundary conditions are presented in Fig. 5. The model has 1800 elements

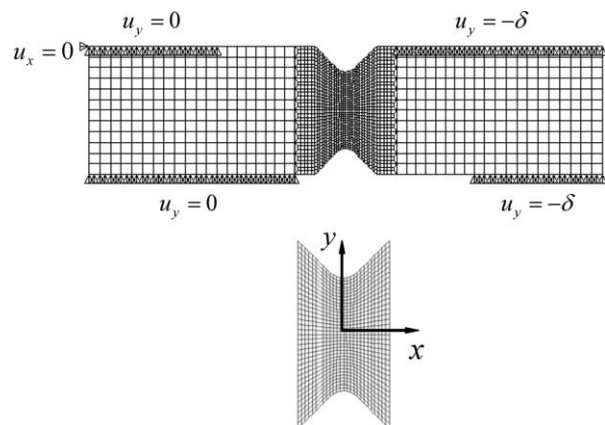


Fig. 5. Mesh and boundary conditions of the Iosipescu specimens.

and 5577 nodes. The nodes along the loading faces of the specimen that are initially in contact with the stationary part of the fixture, have prescribed vertical displacements equal to zero ( $u_y = 0$ ), whereas the horizontal degrees of freedom were left free. Moreover, the upper corner node among this set of nodes, has a horizontal prescribed displacement equal to zero ( $u_x = 0$ ), in order to prevent the free rigid body movement of the specimen in this direction. The nodes belonging to the loading faces of the specimen, initially in contact with the movable part of the fixture, have vertical prescribed displacement equal to  $u_y = -0.1$  mm, and free horizontal degrees of freedom. These boundary conditions are intended to represent the actual loading conditions in the Iosipescu tests [27,29,30].

The numerical shear strain and stress fields are not pure and homogeneous throughout the test section of the specimens in the LR and LT planes. Therefore, global correction factors (CS) are needed to obtain the true shear moduli for these planes. The most heterogeneous fields were obtained for the specimen in the LT plane due to its high orthotropic ratio ( $E_L/E_T = 15$ ). For the specimen in the RT plane, almost homogenous stress and strain states were obtained over a large part of the test section, due to its low orthotropic ratio [27].

From the finite element results, the correction factors  $C$  for the three principal planes were evaluated according to Eq. (4). The global force  $P$  is the sum of all vertical reaction forces in the nodes in contact with the movable part of the fixture. This force represents the load imposed on the specimen and measured by the load cell in the experiments. The correction factors  $S$  were also calculated from the finite element results, using Eq. (5). The engineering shear strain  $\varepsilon_6^{\text{av}}$  was obtained as the average of the engineering shear strains of each node over an area that circumscribes the strain-gauge grid. The correction factors  $C$  and  $S$  obtained for the LR, LT and RT planes, as well as the global correction factors  $CS$ , are shown in Table 2. It was also concluded that the  $CS$  values are insensitive to the initial choice of shear moduli, among the range of the typical variation of wood elastic properties [27].

#### 4.2. Off-axis tensile test models and results

A 2D finite element model was developed for the numerical simulation of the off-axis tensile tests. From the ANSYS finite element library, the quadrilateral

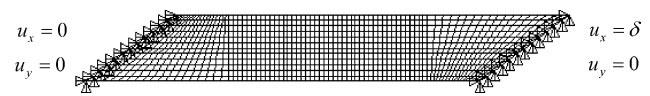


Fig. 6. Mesh and boundary conditions of the off-axis specimens.

isoparametric PLANE182 element was chosen. This element is defined by four nodes with a total of 8 degrees of freedom. Fig. 6 illustrates the finite element mesh, reached after numerical convergence, and the applied boundary conditions. The model has 1053 elements and 960 nodes. The boundary conditions simulate the non-rigid and non-rotating gripping arrangement of the experimental tests. On the nodes of the left face, all the displacements are constrained to zero ( $u_x = 0$  and  $u_y = 0$ ). On the nodes of the right face, the  $u_x$  displacement is fixed to a value 0.5 mm and the  $u_y$  displacement is constrained to zero ( $u_y = 0$ ).

In accordance with previous works [20,21], the numerical results showed that a uniaxial and uniform stress state is obtained throughout the test section of the off-axis specimens, in both LR and LT planes. Therefore, the shear moduli identified experimentally for these planes are thought to be true values, so no correction factors are needed [28].

## 5. Results and discussion

### 5.1. Iosipescu tests

The raw experimental data are illustrated in Fig. 7 for an Iosipescu specimen in the LR plane, where the load reading is plotted against the normal strain gauges readings. It should be noticed that some strain gages had failed before the ultimate failure of the specimens, obstructing the measurement of the ultimate shear strain. However, for all test coupons, the complete load-time curve was recorded, allowing the measurement of maximum applied load. From these data, the average engineering shear strain and the average shear stress were determined according to Eqs. (1) and (2), respectively. In order to suppress parasitic effects due to geometric imperfections of the specimens, the engineering shear strains measured over the two faces of

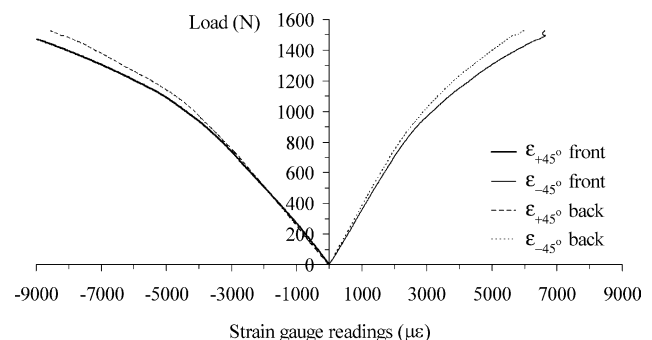


Fig. 7. Typical load vs gauge strain readings, obtained by the Iosipescu tests (LR plane).

Table 2  
Numerical correction factors associated with the Iosipescu tests

Material planes	Numerical correction factors		
	$C$	$S$	$CS$
LR	0.97	0.99	0.95
LT	0.92	0.99	0.91
RT	1.04	0.97	1.01

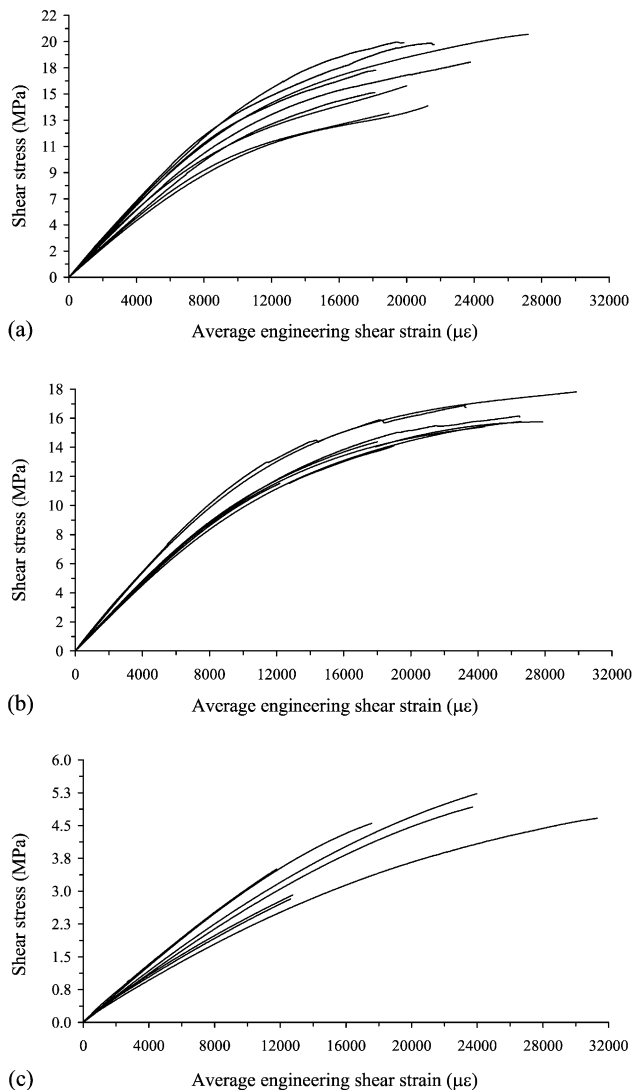


Fig. 8. Apparent shear stress–strain curves obtained by the Iosipescu tests: (a) LR; (b) LT and (c) RT material planes.

the specimens were averaged [12]. The whole set of apparent stress–strain curves are presented in Fig. 8, for the LR, LT and RT specimens. As can be seen, the mechanical response of all specimens is non-linear but it may not represent the intrinsic shear behaviour of wood *Pinus Pinaster Ait.* Indeed, in addition to the material non-linear behaviour, there are other possible sources of non-linearity: geometric and boundary contact non-linearities [30]. From the visual observation of the specimens during the tests, the geometric non-linearity due to the change of fibre orientation, and the boundary contact non-linearity due to the change of the contact lengths between the specimens and the fixture are more apparent for the LR specimens (Fig. 9). These issues were not addressed in the present work.

For the LR and LT specimens, two cracks initiated at the intersection of the notch root and the notch flank (Fig. 9a and b), and slowly propagated parallel to the grain. The RT

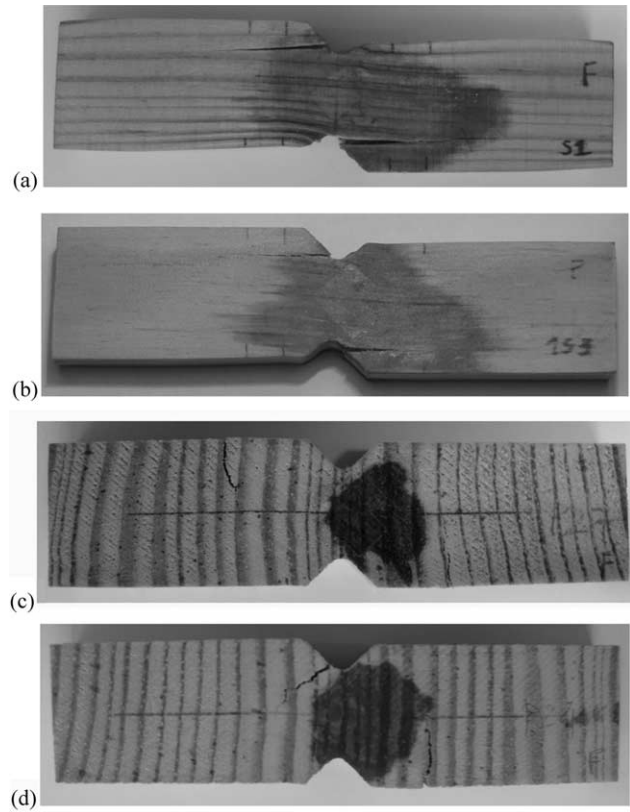


Fig. 9. Typical failures of the Iosipescu specimens: (a) LR; (b) LT; (c) and (d) RT material planes.

specimens failed in a brittle mode, although two families of failures were observed. For one set of specimens, premature cracks developed outside the test section of the specimens, starting at the free surfaces opposite to the inner loading points and propagating along the tangential direction of the wood, at the transition zone between earlywood and latewood (Fig. 9c). For another set of RT specimens, a first crack started near the location of notch root/flank transition and propagated in a typical isotropic mode, at approximately 45° from the horizontal axis of the specimen. Afterwards, a second crack initiated and propagated outside the test section, in the same way as previously described for the first set of specimens (Fig. 9d). Each family of failures in the RT material plane is related to different types of shear response, with quite distinct maximum apparent shear stresses (Fig. 8c).

To determine the apparent shear moduli Eq. (3), the apparent stress–strain curves were fitted with least-squares second order polynomials. The apparent shear moduli were then evaluated as the first derivative of these polynomials, at zero strain. This method was chosen to avoid the difficulty in defining an initial linear zone. The apparent shear moduli, determined at both front and back faces, as well as the apparent average shear moduli, are shown in Fig. 10 for all specimens tested in the LR, LT and RT planes. The scatter of the results obtained from the front and back measurements is in the range of variation usually reported for wood

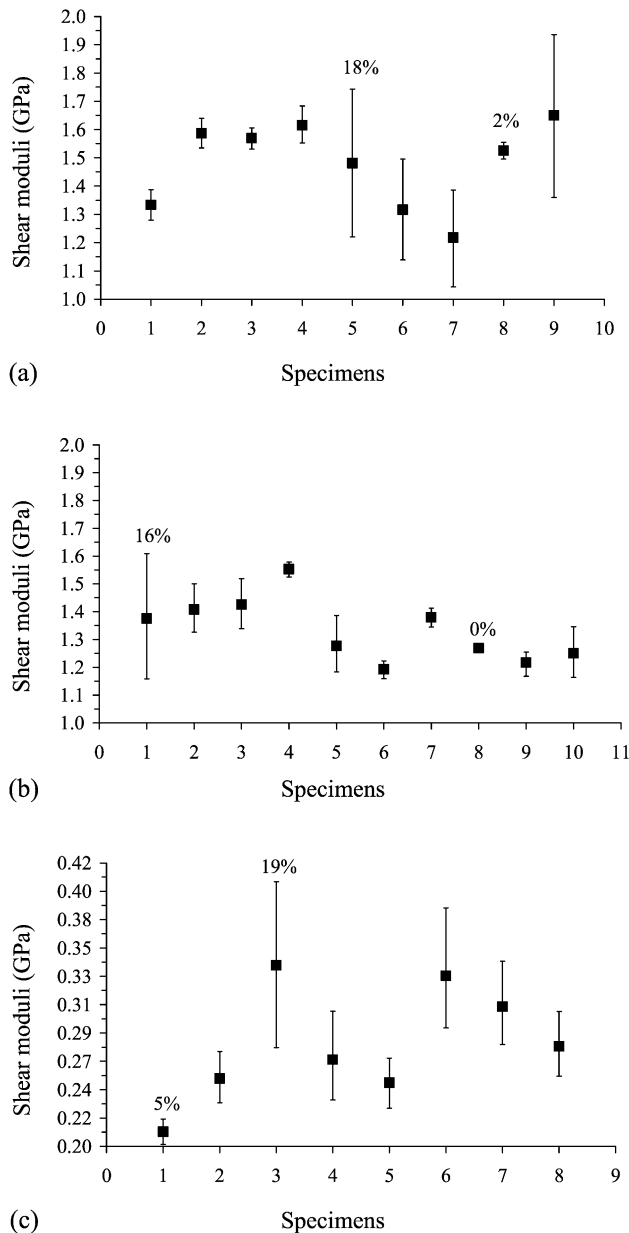


Fig. 10. Front, back and average apparent shear moduli for the Iosipescu specimens: (a) LR; (b) LT and (c) RT material planes.

elastic properties: from 2% up to 18% for LR specimens, from 0% up to 16% for LT specimens, and from 5% up to 19% for RT specimens (Fig. 10). The difference between the measurements in the front and back faces is an intrinsic feature of the Iosipescu test, due mainly to defects in the flatness and parallelism of the loading surfaces of the specimens [12]. A careful observation revealed that the loading surfaces of some LR specimens were composed mainly of latewood (specimens 5, 6, 7 and 9) whereas for other ones they were mainly of earlywood (1–4, 8). This clearly explains the existence of two groups of LR specimens, one of which exhibits face-to-face differences less pronounced than the other one (Fig. 10a). Indeed, loading surfaces made of earlywood are more prone to local

crushing in the earlier stages of loading, improving the uniformity of the load distribution through the thickness and consequently reducing the face-to-face discrepancies. This is consistent with observations made on several types of fibre composite specimens by Pierron [12]. In any case, for all types of specimens, averaging front and back measurements solves the problem [12].

The apparent values of shear modulus were corrected according to Eq. (6), using the numerical factor  $CS$  determined from finite element analyses (Table 2). The corrected shear moduli of each specimen are presented in Table 3, along with the corresponding oven-dry density. After checking the normality of shear moduli distributions using the Shapiro-Wilk test [31], the 95% confidence intervals on the mean values of shear moduli were determined from the  $t$ -distribution (Table 3). Even though the coefficients of variation of shear moduli are in accordance with the dispersion expected for elastic properties of wood, the density was used to explain the inter-specimen variability of shear modulus, assuming a linear relationship between both quantities. Fig. 11 presents the best linear fit obtained between the corrected shear moduli ( $G_{LR}$ ,  $G_{LT}$  and  $G_{RT}$ ) and density. The shear modulus  $G_{LR}$  showed significant correlation (coefficient of correlation  $r^2 = 0.711$ ) at the 95% confidence level with density. On the other hand, at the same level of confidence, density variations poorly explained the variations in the  $G_{LT}$  ( $r^2 = 0.255$ ) and  $G_{RT}$  ( $r^2 = 0.307$ ) shear moduli. It is relevant to mention here that the relationships between shear moduli and density are species dependent, and that very contradictory results were found in the literature about such relationships [32]. However, it must be pointed out that the range of densities obtained in this work is quite narrow ( $0.537$ – $0.623$  g/cm<sup>3</sup>) when compared with the range

Table 3

The oven-dry density ( $d$ ) and corrected shear moduli obtained using the Iosipescu tests

Specimen	LR plane		LT plane		RT plane	
	$d$ (g/cm <sup>3</sup> )	$G_{LR}$ (GPa)	$d$ (g/cm <sup>3</sup> )	$G_{LT}$ (GPa)	$d$ (g/cm <sup>3</sup> )	$G_{RT}$ (GPa)
1	0.561	1.27	0.603	1.26	0.542	0.216
2	0.607	1.52	0.595	1.29	0.551	0.259
3	0.612	1.50	0.590	1.31	0.559	0.348
4	0.605	1.54	0.599	1.42	0.556	0.276
5	0.615	1.42	0.592	1.17	0.548	0.254
6	0.538	1.23	0.581	1.09	0.622	0.345
7	0.537	1.16	0.606	1.26	0.622	0.318
8	0.609	1.46	0.556	1.16	0.623	0.285
9	0.614	1.58	0.574	1.11		
10			0.593	1.15		
MEAN	0.589	1.41	0.589	1.22	0.578	0.286
CI <sup>a</sup>		± 0.112		± 0.073		± 0.039
CV <sup>b</sup> (%)	5.64	10.3	2.56	8.42	6.45	16.2

<sup>a</sup> Confidence intervals (CI) at 95% confidence level.

<sup>b</sup> Coefficient of variation, CV.



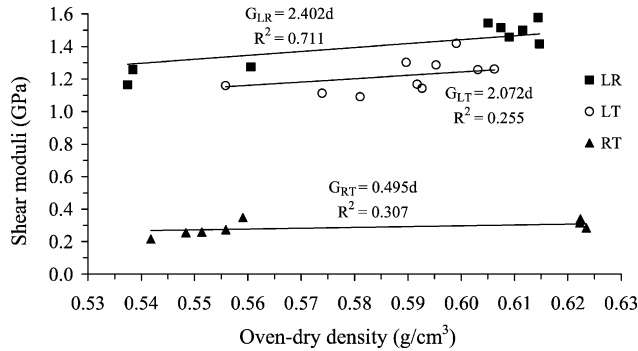


Fig. 11. Shear moduli-density relationship for all principal material planes, obtained using the Iosipescu tests.

considered in those published works, as a consequence of the selection of matched specimens. From the observation of Fig. 11 it seems that  $G_{LR}$  and  $G_{LT}$  are different. Indeed, from the  $t$ -test for equality of means, at a 95% confidence level, it was concluded that the mean values of  $G_{LR}$  and  $G_{LT}$  are different.

The differences between the corrected and apparent shear moduli (which can be recovered from Tables 2 and 3) are lower than the typical coefficient of variation expected for wood elastic properties (4.5, 8.6 and 2.1%, for LR, LT and RT material planes, respectively). As such, the need for employing the correction factor  $CS$  to determine the true shear moduli of wood *Pinus Pinaster Ait.* can be discarded. To reinforce this point, the  $t$ -test for equality of means was applied to the apparent and corrected shear moduli distributions. It was concluded that  $G_{LR}^a$  and  $G_{RT}^a$  give the same properties as  $G_{LR}$  and  $G_{RT}$ , respectively, at a 95% confidence level; on the other hand,  $G_{LT}^a$  and  $G_{LT}$  can be thought to give the same property at a 99% confidence level.

It is well known that the Iosipescu test is not a direct method to determine the shear strength, because failure occurs under a combined stress state [13]. Nevertheless, if the material has a quasi-linear behaviour, an accurate estimation can be obtained from a linear-elastic finite element modelling and from the failure load  $P_f$ , with the help of a proper failure criterion, e.g. the Tsai–Wu criterion for orthotropic materials [33]. This is not the case with the wood *Pinus Pinaster Ait.*, which has a pronounced non-linear shear behaviour in all principal material planes. Because its non-linear constitutive law is not known, the local stress state when failure occurs is inaccessible, hindering the identification of true shear strengths ( $S_{LR}$ ,  $S_{LT}$  and  $S_{RT}$ ). Despite this fact, the average shear stresses for the first crack ( $\sigma_{LR}^{lf}$ ,  $\sigma_{LT}^{lf}$ , and  $\sigma_{RT}^{lf}$ ) and the ultimate average shear stresses ( $\sigma_{LR}^{ult}$ ,  $\sigma_{LT}^{ult}$  and  $\sigma_{RT}^{ult}$ ) were calculated from experimental data according to Eq. (7) (with  $P_f$  equal to the first crack applied load or equal to the maximum load applied during the test, respectively), and presented in Table 4.

As described above, the first cracks in the LR and LT specimens occur at the notch root/flank intersection, where, according to the results of the finite element analyses, there

Table 4

First crack and ultimate average shear stresses identified using the Iosipescu tests

Specimen	LR plane		LT plane		RT plane	
	$\sigma_{LR}^{lf}$ (MPa)	$\sigma_{LR}^{ult}$ (MPa)	$\sigma_{LT}^{lf}$ (MPa)	$\sigma_{LT}^{ult}$ (MPa)	$\sigma_{RT}^{lf}$ (MPa)	$\sigma_{RT}^{ult}$ (MPa)
1	14.4	14.9	15.4	16.6	2.38	3.29
2	12.6	16.3	14.7	19.0	2.76	3.88
3	17.2	18.6	15.5	17.3	0.97	4.16
4	16.2	17.9	14.5	18.6	2.86	3.36
5	19.1	19.1	16.1	17.3	4.65	4.65
6	13.2	13.8	16.5	18.1	1.01	4.62
7	14.9	15.0	19.1	20.6	1.16	5.63
8	15.9	16.8	16.0	17.5	3.27	5.18
9	19.5	19.5	14.7	18.1		
10			16.1	18.1		
MEAN	15.9	16.9	15.9	18.1	2.38	4.35
CI <sup>a</sup>	$\pm 1.857$	$\pm 1.567$	– <sup>b</sup>	$\pm 0.786$	$\pm 1.081$	$\pm 0.696$
CV <sup>c</sup> (%)	15.2	12.1	8.4	6.1	54.3	19.2

<sup>a</sup> Confidence intervals (CI) at 95% confidence level.

<sup>b</sup>  $\sigma_{LT}^{lf}$  does not follow a normal distribution.

<sup>c</sup> Coefficient of variation, CV.

is a combined stress state with concentrations; in addition, the transverse normal stresses (perpendicular to the longitudinal material direction) at this location are tensile. Furthermore, even though the type of wood failure corresponding to the maximum average shear stresses is not clear, it occurs at the test section of the specimens under a combined stress state with compressive transverse stresses. In view of these observations and in agreement with what was found for unidirectional composite materials by Pierron and Vautrin [13,14], it is likely that the first crack average shear stresses and the ultimate average shear stresses are lower and upper bounds, respectively, of the true shear strengths of wood ( $S_{LR}$  and  $S_{LT}$ ). Assuming the validity of this hypothesis, because the lower and upper bounds are very close (Table 4), we can conclude that the Iosipescu shear test method give a good estimation of shear strengths of wood for the LR and LT principal material planes, even without using any failure criterion.

The RT specimens exhibited two types of failures, presented above (Fig. 9c and d). The occurrence of an initial crack at the free surfaces opposite to the inner loading points is related to the existence of large tensile longitudinal stresses (of the same order of magnitude of the average shear stress) as revealed by the finite element analyses. The other initial failure location, also anticipated by the finite element analyses, is the notch root/flank intersection, where a stress concentration effect exists. Which one of these failures is the first one to occur in a particular specimen, is obviously dependent on the random spatial distribution of defects, mainly resin channels, which are more frequent at the transition zone between earlywood and latewood [32]. Hence, it is not surprising the greater scatter of  $\sigma_{RT}^{lf}$  values and the larger difference between these and the values of the ultimate average shear stress ( $\sigma_{RT}^{ult}$ ). If the ultimate average

shear stress is an accurate estimation of shear strength of wood for this particular material plane, is an issue that must be examined by comparison with an independent test method.

Applying the *t*-test for equality of means, it was verified that the maximum shear stresses for LR and LT planes are equal, at a 95% confidence level. Although the  $\sigma_{LT}^{lf}$  distribution does not follow a normal distribution, it is apparent from the results of Table 4 that it is equal to  $\sigma_{LR}^{lf}$ . Therefore, we can conclude that wood *Pinus Pinaster Ait.* has the same shear strength in the LR and LT principal material planes. However, the shear strength for the RT material plane is quite distinct (Table 4).

### 5.2. Off-axis tests

In Fig. 12, the applied load was plotted as a function of the strains measured with the individual gauges of the rosette, for an off-axis LR specimen. These curves are representative of typical experimental data from the off-axis tensile tests. Because most of the strain rosettes had ceased to perform properly before the ultimate failure of the specimens, the maximum shear strain was not measured. However, like for the Iosipescu test, the complete load-time curves were recorded. The shear stress–strain curves were derived from these data, calculating the engineering shear strains and the shear stresses through Eqs. (8) and (9), respectively. All the LR and LT specimens exhibited non-linear shear behaviour, as can be seen in Fig. 13.

The typical failure modes observed in the off-axis tensile tests are shown in Fig. 14. Fracture occurred in the gauge section, along the grain direction and away from the end-tabs. Therefore, failure was free from any stress concentration effects and, according to the results of finite element analyses, occurred under an almost homogeneous and uniaxial stress state.

The identification of shear moduli was made directly from the shear stress–strain relationships, without using any correction factor. As was done in the Iosipescu tests, the shear stress–strain curves were first fitted with least-squares second order polynomials, and the shear moduli were then

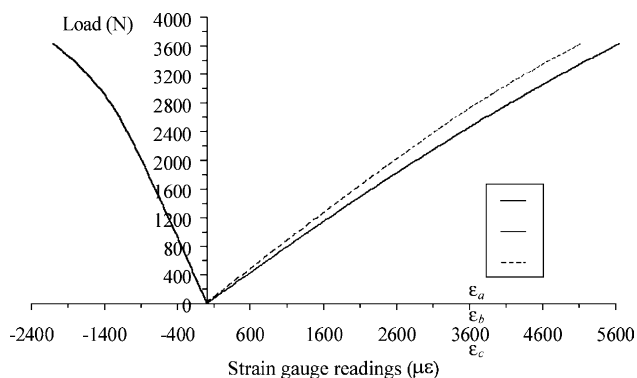


Fig. 12. Typical load vs gauge strain readings, obtained using the off-axis tests (LR plane).

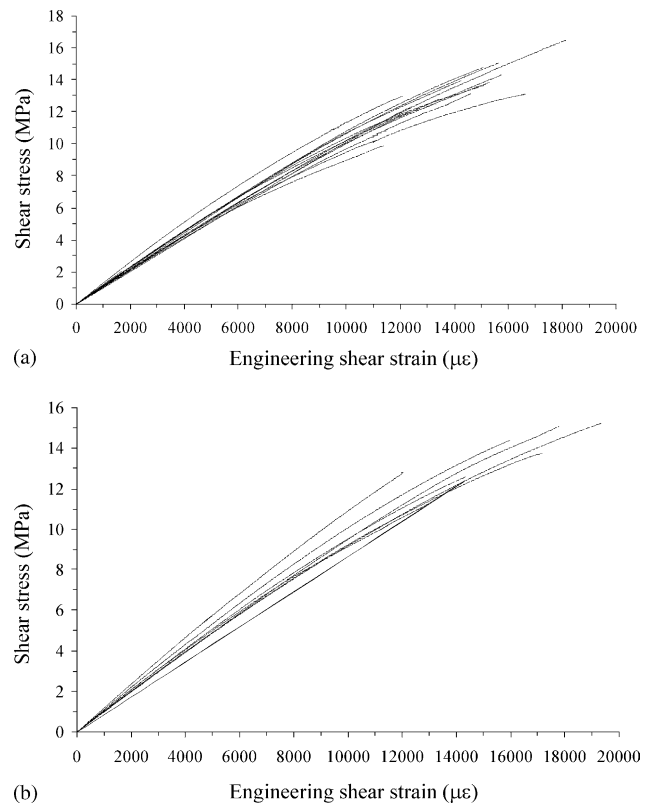


Fig. 13. Complete shear stress–strain apparent curves obtained using the off-axis tests: (a) LR and (b) LT material planes.

evaluated as the first derivative of those polynomials, at zero shear strain. The results of such procedure are presented in Table 5, along with the oven-dry density of each specimen. Once verified the normality assumption of each shear moduli distributions, the confidence intervals over the mean values were determined, at a 95% confidence level (Table 5). The relatively low coefficients of variations of density distributions (4.04% for LR specimens and 4.01% for LT specimens) are in agreement with the selection of matched specimens. Probably due to this fact, the scatter of  $G_{LR}$  (coefficient of variation  $cv = 7.00\%$ ) and  $G_{LT}$  ( $cv = 8.12\%$ ) are lower than the scatter of elastic properties of wood usually reported in the literature [26,32].

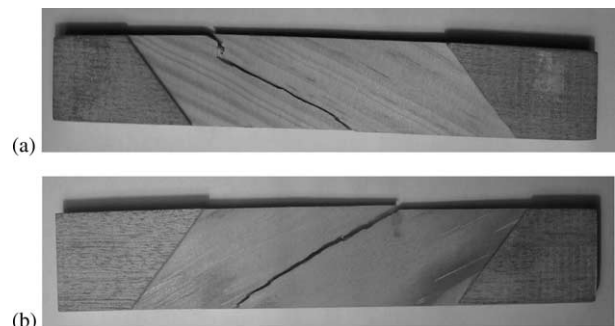


Fig. 14. Typical failures of the off-axis specimens: (a) LR and (b) LT material planes.

Table 5  
The oven-dry density ( $d$ ) and the shear modulus obtained using the off-axis tests

Specimen	LR plane		LT plane	
	$d$ (g/cm <sup>3</sup> )	$G_{LR}$ (GPa)	$d$ (g/cm <sup>3</sup> )	$G_{LT}$ (GPa)
1	0.630	1.23	0.552	1.04
2	0.609	1.14	0.527	1.00
3	0.579	1.03	0.532	1.01
4	0.616	1.11	0.543	0.98
5	0.586	1.13	0.532	1.18
6	0.566	1.05	0.547	1.10
7	0.566	1.10	0.592	1.24
8	0.560	1.09	0.531	0.95
9	0.570	1.10	0.534	0.98
10	0.564	1.03	0.501	1.10
11	0.564	1.06	0.516	1.02
12	0.574	1.02	0.527	1.00
13	–	1.32	0.562	1.04
14	–	1.17	0.534	0.95
15	–	1.11		
16	–	1.15		
MEAN	0.582	1.11	0.538	1.04
CI <sup>a</sup>		± 0.042		± 0.049
CV <sup>b</sup> (%)	4.044	7.00	4.010	8.12

<sup>a</sup> Confidence intervals (CI) at 95% confidence level.

<sup>b</sup> Coefficient of variation, CV.

The shear modulus distributions for the LR and LT samples were compared in order to verify if they came from the same population, using the  $t$ -test for equality of means. The results show that the mean values of  $G_{LR}$  and  $G_{LT}$  are different at 95% of confidence level, although they were found similar at a 99% of confidence level. It is worthy to take note that the greater mean value of  $G_{LR}$  corresponds to a greater mean value of density. Hence, it is necessary to verify if the difference between the mean values of the two shear modulus (at a 95% confidence level) is due to density variations. In Fig. 15, the experimental values of shear moduli were plotted against the measured values of density, from both LR and LT samples. Assuming a linear relationship between both quantities [32], it was found by

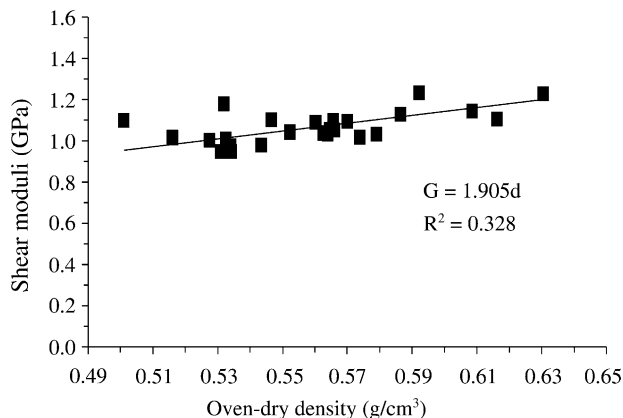


Fig. 15. The shear moduli–density relationship, taking all specimens tested using the off-axis tests.

regression analysis that the variations of density explained only about 32.8% of the variations of the shear modulus, at a 95% confidence level. This non-significant correlation allows us to conclude that the mean values of  $G_{LR}$  and  $G_{LT}$ , determined from the off-axis tensile test, are inherently different properties (at a 95% confidence level).

As mentioned above, the use of oblique end tabs enabled the failure of off-axis coupons under a state of homogeneous stress field. The stress components in the principal material directions when failure occurs can then be determined from the failure load  $P_f$  and from the well-known transformation law of the stress tensor Eq. (9). The ultimate shear stress of each test coupon ( $\sigma_{LR}^{ult}$  and  $\sigma_{LT}^{ult}$ ) calculated by this way is shown in Table 6. Because the stress state is not pure shear, the off-axis tensile test does not provide a direct identification method of the material shear strength, i.e. the ultimate shear stress cannot be considered the true shear strength and a suitable strength criterion must be used to extrapolate this property. To properly account for the presence of transverse tensile stresses, Pierron and Vautrin [21] had employed the Tsai–Wu failure quadratic criterion. In this work, due to the lack of data about compression strengths of wood *Pinus Pinaster Ait.*, the Tsai–Hill failure criterion [33] was used

$$\frac{\sigma_1^2}{X^2} - \frac{\sigma_1 \sigma_2}{XY} + \frac{\sigma_2^2}{Y^2} + \frac{\sigma_6^2}{S^2} = 1. \quad (12)$$

In this equation,  $X$  is the strength parallel to the grain (also denoted  $X_L$ ),  $Y$  represents the strength perpendicular to the grain (denoted  $Y_R$  in the radial direction and  $Y_T$  in the tangential direction).

Table 6  
The ultimate shear stresses and the shear strengths determined using the Tsai–Hill failure criterion, obtained from the off-axis tests

Specimen	LR plane		LT plane	
	$\sigma_{LR}^{ult}$ (MPa)	$S_{LR}$ (MPa)	$\sigma_{LT}^{ult}$ (MPa)	$S_{LT}$ (MPa)
1	13.8	15.9	11.2	14.5
2	13.0	14.6	15.2	18.2
3	12.5	14.0	13.7	15.8
4	10.7	11.5	15.3	18.3
5	14.8	18.0	12.8	14.5
6	13.3	15.2	14.4	17.0
7	13.7	15.9	14.0	16.2
8	17.2	21.8	16.2	20.0
9	15.2	18.2	15.8	19.3
10	14.3	16.8	13.6	15.7
11	13.1	14.9	13.3	15.3
12	13.9	16.1	14.5	17.1
13	13.8	16.0	12.7	14.3
14	16.5	20.7	13.8	16.0
15	12.5	14.0		
16	16.6	20.7		
MEAN	14.1	16.5	14.0	16.6
CI <sup>a</sup>	± 0.9	± 1.5	± 0.8	± 1.0
CV <sup>b</sup> (%)	12.1	16.7	9.5	10.9

<sup>a</sup> Confidence intervals (CI) at 95% confidence level.

<sup>b</sup> Coefficient of variation, CV.

the tangential direction) and  $S$  represents the shear strength (denoted  $S_{LR}$  and  $S_{LT}$  in the LR and LR planes, respectively). The values of  $X_L$ ,  $Y_R$  and  $Y_T$  for wood *Pinus Pinaster Ait.* measured at the laboratory [25], are

$$X_L = 97.5 \text{ MPa}, Y_R = 7.9 \text{ MPa and } Y_T = 4.2 \text{ MPa.} \quad (13)$$

The values of the different stress components are derived from the failure load  $P_f$  and from Eq. (9). The shear strength values derived in this way are presented in Table 6 for each test coupon. As expected, the ultimate shear stresses are lower than the shear strengths, but very close to each other. Thus, the off-axis tensile test gives an accurate lower bound of shear strength of wood *Pinus Pinaster Ait.*, for both LR and LT material planes, directly from the measured failure load.

Applying the  $t$ -test for equality of means, it was concluded, at a 95% confidence level, that the shear strength is the same in the LR and LT material planes. Different authors have pointed out that a good correlation exists between density and strength properties of wood [32]. In this work, a similar conclusion was not achieved for the shear strength and density values obtained by the off-axis tests. This result may be attributed to the narrow range of density values, in accordance with the selection of matched specimens.

### 5.3. Comparison between the Iosipescu and the off-axis tests

In this section, a comparison between the Iosipescu and off-axis test methods will be made in terms of shear moduli and shear strengths of wood *Pinus Pinaster Ait.* No attempt was made to compare the full non-linear stress–strain curves extracted from both test methods, on the framework of a suitable non-linear constitutive law, e.g. the Sun and Chen plasticity model [34]. This will be the subject of future work.

It appears clearly from Tables 3 and 5 that a very good reproducibility of mean densities was achieved through the selection of matched samples, except for the off-axis LT specimens. In any case, as demonstrated before, the shear moduli can be assumed to be independent of density, for the range of experimental data acquired in this work. As a consequence, it is admissible to make a comparative evaluation of the Iosipescu and off-axis shear test method, concerning the shear moduli and shear strength identification.

The first conclusion arising from the results of Tables 3 and 5 is that the scatter of shear moduli for the Iosipescu samples is of the same order of magnitude as for the off-axis samples, although the latter is slightly lower than the first, which is consistent with the fact that the volume tested is smaller for the Iosipescu specimen than for the off-axis one, so that the latter will be less sensitive to material heterogeneity. Another point that arises from these results is that the mean shear moduli extracted from the Iosipescu shear tests are always higher than the mean values extracted

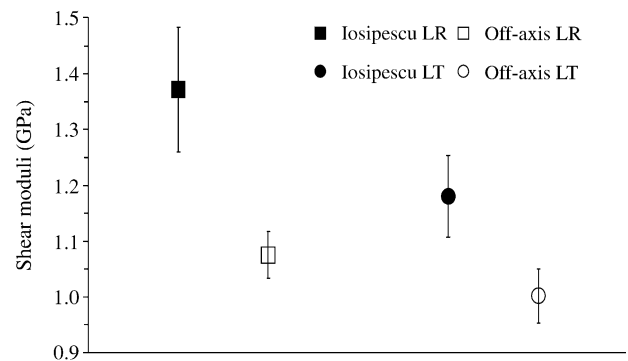


Fig. 16. Confidence intervals over the shear moduli identified using the Iosipescu and off-axis tests, in the LR and LT material planes.

from the off-axis tensile test. This point is reinforced when the 95% confidence intervals of the mean values are also compared (Tables 3 and 5, and Fig. 16). Applying the  $t$ -test for equality of means, it was concluded that at a 95% confidence level a significant difference exists between the shear moduli determined from the Iosipescu and from the off-axis tests, for both LR and LT material planes. The shear modulus  $G_{LR}$  derived from the Iosipescu test is higher by about 26%, whereas the shear modulus  $G_{LT}$  is higher by about 17%.

Pierron et al. [35] observed that the shear modulus of an isotropic material (PMMA) measured with the Iosipescu test was higher by about 3% than the shear modulus measured with a tensile test. They argued that the systematic difference between the two test methods was probably to be attributed to the inaccuracy of the correction factors employed in the Iosipescu test, determined by finite element modelling. However, this argument can not explain the differences found in this work for  $G_{LR}$  and  $G_{LT}$  between the Iosipescu and off-axis tests. At present, the only explanation that the authors can think of to account for the differences in shear moduli obtained by the two tests is that the material may not be orthotropic. Indeed, since neither tests give rise to pure shear, the presence of extension/shear coupling terms in the compliance matrix would invalidate Eq. (3). Nevertheless, this explanation should be confirmed experimentally by on-axis tests on LR or LT specimens to check for the presence of shear strains.

From the data presented in Tables 4 and 6, and also shown in Fig. 17, it can be seen that the average values of ultimate shear stresses measured on the off-axis specimens are lower by about 13% than the average values of the first crack shear stresses registered on the Iosipescu specimens. Because the first failure in Iosipescu specimens are due to stress concentrations, a greater value would be expected for the maximum shear stresses obtained from the off-axis test, however both results are very consistent. Moreover, the shear strengths ( $S_{LR}$  and  $S_{LT}$ ) evaluated from the off-axis test by using the Tsai–Hill failure criterion are between the lower and upper bounds of shear strengths estimated directly from the experimental data of Iosipescu test.



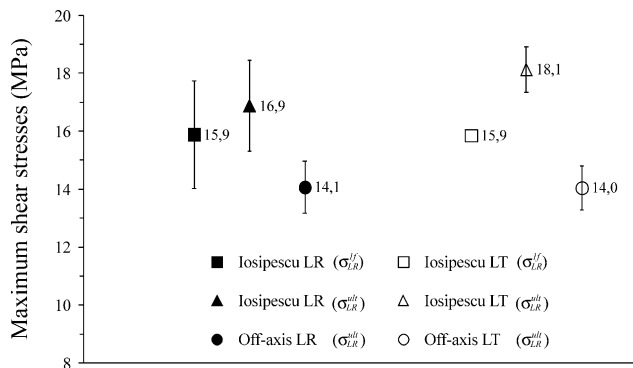


Fig. 17. Confidence intervals over the first crack and ultimate average shear stresses identified using the Iosipescu and off-axis tests, in the LR and LT material planes.

Consequently, the authors think that both shear test methods are similarly valuable for the evaluation of shear strengths of wood, at least for the LR and LT principal material planes.

In comparison with the Iosipescu shear test method, the weak point of the off-axis tensile test is that it is not applicable to the RT plane, mainly because this plane is almost an isotropy plane. Nevertheless, the shear properties are less important to identify in this plane because of near-isotropy.

The experimental values of the shear properties presented in this work should not be regarded as allowable properties of wood *Pinus Pinaster Ait.* A much larger experimental study would be needed in order to establish such characterization, which was out of scope in this work. Nevertheless, the authors are convinced of the validity of the conclusions regarding the relative merits of the Iosipescu and off-axis test methods for accurate characterization of the shear behaviour of wood.

## 6. Conclusion

In this paper, was examined the applicability of the Iosipescu and off-axis test methods for the identification of the shear response of wood *Pinus Pinaster Ait.* All the orthotropic material planes (LR, LT and RT) have been considered. The data reduction and testing methodologies for both test methods have been presented. Finite element correction factors are given for the LR, LT and RT Iosipescu specimens, to account for the heterogeneity of the stress and strain fields.

The off-axis tensile test is not valid for the RT plane of wood, mainly because this natural symmetry plane is almost isotropic. In principle, the Iosipescu test can be used to determine the shear properties of wood *Pinus Pinaster Ait.* for all principal material planes, without using any correction factor, although its applicability for the RT plane need to be further investigated.

It was shown that the Iosipescu and 15° off-axis tests provide different shear moduli values. This is believed to be a consequence of possible material extension/shear coupling, i.e. the material is not orthotropic in its natural symmetry axes, but this needs to be confirmed with additional experimental evidence.

It was demonstrated that the Iosipescu test allows the direct measurement of lower and upper bounds of shear strengths, which are very close to each other on the case of LR and LT planes. On the other hand, the off-axis test gives accurate lower limits of those shear strengths, directly from the measured failure loads.

The statistical processing of data revealed that the LR and LT shear moduli of wood *Pinus Pinaster Ait.* are different. However, the shear strengths seem to be the same for the LR and LT material planes.

## Acknowledgements

We would like to thank Patrick Ghidossi for his help in the preliminary Iosipescu tests and José Luis Louzada in his help in the preparation of the specimens. We would also like to thank the Foundation for Science and Technology for the financial support of this work, in the framework of the project 'Non-linear mechanical behaviour of wood' (POC-TI/36270/EME/2000).

## References

- [1] Cheung CK, Sorensen HC. Effect of axial loads on radial stress in curved beams. *Wood Fiber Sci* 1983;15(3):263–75.
- [2] Zalph BL, McLain TE. Strength of wood beams with fillet interior notches: a new model. *Wood Fiber Sci* 1992;24(2):204–15.
- [3] Bouchair A, Vergne A. An application of Tsai criterion as a plastic flow law for timber bolted modeling. *Wood Sci Technol* 1995;30(1):3–19.
- [4] Zandberg JG, Smith FW. Finite element fracture prediction for wood with knots and cross grain. *Wood Fiber Sci* 1988;20(1):97–106.
- [5] Pellicane PJ, Franco N. Modeling wood pole failure. Part 1: finite element stress analysis. *Wood Sci Technol* 1994;28(3):219–28.
- [6] Yoshihara H, Ohsaki H, Kubojima Y, Ohta M. Applicability of the Iosipescu shear test on the measurement of the shear properties of wood. *J Wood Sci* 1999;45:24–9.
- [7] Iosipescu N. New accurate procedure for single shear testing of metals. *J Mater* 1967;2(3):537–66.
- [8] Walrath DE, Adams DF. The Iosipescu shear test as applied to composite materials. *Exp Mech* 1983;23(1):105–10.
- [9] Adams DF, Walrath DE. Further developments of the Iosipescu shear test method. *Exp Mech* 1987;27(2):113–9.
- [10] ASTM D 5379-93, Test method for shear properties of composite materials by the V-notched beam method. Philadelphia, PA: American Society for Testing and Materials; 1993.
- [11] Pierron F. New Iosipescu fixture for the measurement of the in-plane shear modulus of laminated composites: design and experimental procedure. Technical report, No. 940125, Ecole des Mines de Saint-Etienne, 1994.
- [12] Pierron F. Saint-Venant effects in the Iosipescu specimen. *J Compos Mater* 1998;32(22):1986–2015.

- [13] Pierron F, Vautrin A. Measurement of the in-plane shear strength of unidirectional composites with the Iosipescu test. *Compos Sci Technol* 1997;57(12):1653–60.
- [14] Pierron F, Vautrin A. New ideas on the measurement of the in-plane shear strength of unidirectional composites. *J Compos Mater* 1997; 31(9):889–1997.
- [15] Dumail J-F, Olofsson K, Salmén L. An analysis of rolling shear of spruce wood by the Iosipescu method. *Holzforschung* 2000;54(4): 420–6.
- [16] Yoshihara H, Ohsaki H, Kubojima Y, Ohta M. Comparisons of shear stress/shear strain relations of wood obtained by Iosipescu and torsion tests. *Wood Fiber Sci* 2001;33(2):275–83.
- [17] Liu JY. Effects of shear coupling on shear properties of wood. *Wood Fiber Sci* 2000;32(4):458–65.
- [18] Chamis CC, Sinclair JH. Ten-deg off-axis test for shear properties in fiber composites. *Exp Mech* 1977;17:339–46.
- [19] Pindera M-J, Herakovich CT. Shear characterization of unidirectional composites with the off-axis tension test. *Exp Mech* 1986;26(1): 103–12.
- [20] Sun CT, Chung I. An oblique end-tab design for testing off-axis composite specimens. *Composites* 1993;24(8):619–23.
- [21] Pierron F, Vautrin A. The 10° off-axis tensile test: a critical approach. *Compos Sci Technol* 1996;56(4):483–8.
- [22] Kawai M, Morishita M, Satoh H, Tomura S, Kemmochi K. Effects of end-tab shape on strain field of unidirectional carbon/epoxy composite specimens subjected to off-axis tension. *Compos Part A* 1997;28A: 267–75.
- [23] Yoshihara H, Ohta M. Estimation of the shear strength of wood by uniaxial-tension tests of off-axis specimens. *J Wood Sci* 2000;46: 159–63.
- [24] Liu JY. Analysis of off-axis tension test of wood specimens. *Wood Fiber Sci* 2002;34(2):205–11.
- [25] Pereira JL. Mechanical behaviour of wood *Pinus Pinaster Ait.* in traction on the material directions. MSc Thesis, University of Trás-os-Montes e Alto Douro, Vila Real, Portugal; 2004. In Portuguese.
- [26] Forest Products Laboratory. Wood Handbook-Wood as an Engineering Material. Gen. Tech. Rep. FPL-GTR-113, US Department of Agriculture, 1999.
- [27] Xavier JC. Identification of the shear behaviour of wood *Pinus Pinaster Ait.* by the Iosipescu shear test. MSc Thesis, University of Trás-os-Montes e Alto Douro, Vila Real, Portugal; 2003. In Portuguese.
- [28] Garrido NM. Identification of the shear behaviour of wood *Pinus Pinaster Ait.* by the off-axis tensile test. MSc Thesis, University of Trás-os-Montes e Alto Douro, Vila Real, Portugal, (in preparation). In Portuguese.
- [29] Pierron F. L'essai de cisaillement plan d'Iosipescu: modélisation et méthodologie expérimentale pour les composites. PhD thesis, University of Lyon I, France, 1994. In French.
- [30] Ho H, Tsai MY, Morton J, Farley GL. Numerical analysis of the Iosipescu specimen for composite materials. *Compos Sci Technol* 1993;46:115–28.
- [31] Neuilly M. Modelling and estimation of measurement errors. Lavoisier Publishing, Paris; 1999.
- [32] Dinwoodie JM. Timber: its nature and behaviour. Routledge mot EF. and Spon N, 2000.
- [33] Tsai SW, Hahn HT. Introduction to composite materials. Technomic Publishing CO, Lancaster; 1980.
- [34] Sun CT, Chen JL. A simple flow rule for characterizing nonlinear behavior of fiber composites. *J Compos Mater* 1989; 23:1009–20.
- [35] Pierron F, Vautrin A, Harris B. The Iosipescu in-plane shear test: validation on an isotropic material. *Exp Mech* 1995;35(2):130–6.